Implementation of the response to synchronization in e-puck2 robots

Tomaselli, Cinzia; Ramírez-Ávila, Gonzalo Marcelo; Gambuzza, Lucia Valentina; Frasca, Mattia; Tuci, Elio; Carletti, Teo

Published in:
Artificial Life and Evolutionary Computation - 18th Italian Workshop, WIVACE 2024, Revised Selected Papers

DOI:
10.1007/978-3-031-93631-9

Publication date:
2025

Document Version
Peer reviewed version

Implementation of the response to synchronization in e-puck2 robots

Cinzia Tomaselli[1 [0000−0002−2632−7517]], Gonzalo Marcelo Ramírez-Ávila[2,4,5 [0000−0003−4522−9012]], Lucia Valentina Gambuzza[1 [0000−0002−5859−285X]], Mattia Frasca[1 [0000−0002−4361−0576]], Elio Tuci[3,4 [0000−0001−7345−671X]], and Timoteo Carletti[2,4 [0000−0003−2596−4503]]

[1] Department of Electrical, Electronic and Computer Science Engineering, University of Catania, Italy
[2] Department of Mathematics, University of Namur, Belgium
[3] Department of Computer Science, University of Namur, Belgium
[4] Namur Institute for Complex Systems, naXys, University of Namur, Belgium
[5] Instituto de Investigaciones Físicas, & Planetario Max Schreier, Universidad Mayor de San Andrés, La Paz, Bolivia
timoteo.carletti@unamur.be

Abstract. The response to synchronization is a phenomenon observed in several firefly species, where male ensembles synchronize their rhythmic flashes by triggering a response from females which ends the courtship process. In this work, we present a robotic implementation of this phenomenon by using a team of static e-puck2 robots that integrate oscillatory dynamics to mimic the flashing rhythm of the fireflies. To this end, robots communicate with each other via infrared (IR) and follow a distributed control law. They are divided into two groups: one representing the male population with bursting dynamics and the other representing females with non-bursting behavior. Our experimental results demonstrate that response to synchronization is robust with respect to the presence of realistic features such as obstacles and information loss. These factors play a significant role in refining the original model and enhancing its applicability in real-world scenarios.

Keywords: Coupled oscillators · bursty oscillators · E-puck robots · Synchronization.

1 Introduction

Synchronization is the phenomenon according to which coupled (similar) self-sustained oscillators self-organize their rhythms to exhibit an (almost) unison rhythm without the need of any external control [28]. It is a widespread emerging phenomenon resulting from the interaction among individual oscillators [3, 4]. It is found in the synchronous communication in several animals emitting sound as frogs [1], katydids [25] and cicadas [11], or communicating by other mechanical signals as in the case of crabs [2], just to mention a few. One of the most interesting examples of synchronization in animals is the phenomenon observed in

several firefly species [6]. This has inspired numerous studies focused on modeling fundamental aspects of flashing behavior [22, 20, 26] or designing electronic circuits that mimic such behavior [17, 12]. Although simultaneous firefly flashing is a paradigmatic example of synchronization [5, 8, 32, 34] and is related to mating and courtship [18, 5, 10], most of the research focused on male synchronization as the main factor of courtship, and few works considered the role of the female [24, 9, 29]. In some works, flash emission from females has been studied as predatory behavior to chase males of other species [38, 19]. Other studies have explored the female response to controlled flash sequences that mimic the flashing pattern of conspecific males [7, 21, 23], revealing that females are sensitive to male signals, i.e., the female response is triggered or enhanced by male synchronization. This phenomenon is known as the *response to synchronization* [31].

This phenomenon is present in several firefly species in which the male and female rhythmic features might be quite different [14, 33], among these species there is the genus *Photinus carolinus* [13]. Firefly courtship in several species consists thus of male synchronization followed by the female response, whose flashing pattern might exhibit simultaneous flashing or some other ordered flashing patterns. It is noteworthy to point out that groups of females cannot give rise to ordered flashing patterns without the presence of males.

The response to synchronization is described by the mathematical model discussed in [30] which considers dissimilar oscillators, one type of which is not capable of synchronizing without the presence of the second group. The purpose of this work is the experimental validation of this model using a team of e-puck2 robots. The robotic implementation, indeed, allows for testing the model's robustness against real-world factors such as message loss and the presence of obstacles that may affect neighborhood detection.

Our approach aligns with previous studies that implemented mathematical models of complex systems using robots, such as kilobots for naming game [37], or Elisa-3 robots for exploring collective dynamics through decentralized control [35, 36]. In this context, synchronization has been explored under various scenarios. For instance, [16] explores a swarm of synchronized robots emitting pulses during navigation, with robots near a target increasing their oscillation frequency to induce the others to follow them. Another example is [27] which investigates synchronization in mobile pulse-coupled oscillators inspired by fireflies behavior, revealing that synchronization behaviors depend on agent speed and interaction parameters, leading to slow, fast, or inhibited synchronization regimes. Additionally, [35] considers a system of randomly moving robots, each integrating a Rössler oscillator and coupled with nearby units to reach synchronization.

For the purpose of this work, each robot will be endowed with an internal dynamic describing a non-smooth oscillator "producing a flash" during the discharging stage that enables communication with other robots and consequently mimics the flashing behavior of a *Photinus carolinus* firefly male or female. We show that interacting "male" robots are able to synchronize while interacting "female" robots cannot; however, when the "females" are mingled with the "male"

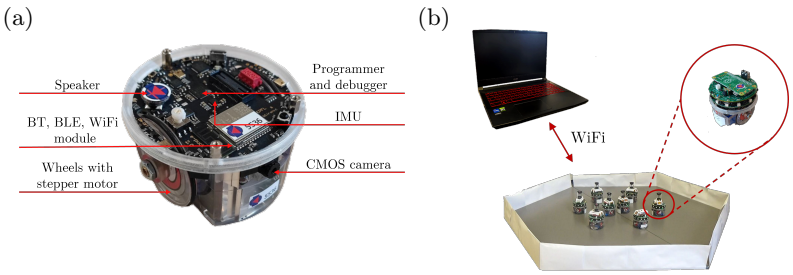

Fig. 1. (a) The *e-puck2* robot. (b) The experimental setup.

robots, the former can respond to the synchronized signal received by the males and produce regular temporal patterns. Then, the experimental results are compared and complemented with the analysis of the non-smooth differential equations model implemented to describe the interaction of simulated populations of "male" and "female" robots whose internal dynamics mimic the firefly pulsating pattern. As a first preliminary investigation of the experimental setup and the role of the model parameters, we decided to keep the robots at fixed positions. The more general framework of moving robots will be presented in a forthcoming companion paper.

A relevant result of our work is that realistic conditions do not impede the response to synchronization phenomenon, proving the robustness of the model. In addition, the findings from our work might endow the model with essential aspects for more realistic situations. The latter can be useful for practical applications and for improving simulation features.

The paper is organized as follows. In Sec. 2, we describe the basic characteristics of the robots and the experimental setup. The model, its features, and its implementation in e-puck robots are detailed in Secs. 3 and 4. The experimental results and their interpretation are given in Sec. 5 and finally, we give the conclusions and perspectives of the work.

2 Description of the robots and experimental setup

The experiments have been carried out using *e-puck2* robots equipped with the *Pi-puck* extension (see `https://www.gctronic.com/e-puck2.php`). Each of these robots has a cylindrical body characterized by a diameter of $d = 7\,[cm]$, a height of $h = 5.5\,[cm]$, and a weight of $w = 150\,[g]$. It can move on a flat surface using a differential drive system with two wheels powered by stepper motors. Each robot is equipped with several sensors, shown in Fig. 1(a). For the experiment described in this paper, we only use the range and bearing board (more details at `https://www.gctronic.com/doc/index.php?title=Others_Extensions#Range_and_bearing`). This is a circular board featuring 12 IR emitters and 12 IR receivers uniformly distributed along its circumference, providing a decentralized communication system based on infrared technology with frequency modulation. This allows the robots to send messages of two bytes at a

frequency of approximately $40\,[Hz]$ and to determine the range and bearing of the transmitter at distances of up to about $d_M = 1\,[m]$, which can be tuned by adjusting the transmission power of the infrared transmitters.

The experimental setup, shown in Fig. 1(b), consists of N robots placed in an arena of hexagonal shape, with each side measuring $l = 60\,[cm]$. The setup also includes a local computer that communicates with the robots via WiFi to initiate experiments and collect data from them at the end of each experiment.

3 The model

In [30], both male and female fireflies are modeled as oscillators that alternate between an active stage, during which they oscillate, and a resting stage, during which they remain inactive and do not respond to external inputs. Males are represented by bursting oscillators (BOs), which exhibit a series of rapid oscillations (bursts of spikes) for each active stage, while females are modeled as non-bursting oscillators (NBOs), showing a single oscillation per active stage. Each oscillation consists of a charge and discharge stage whose duration is influenced by interactions with other units. However, the resting stage has a constant duration as it is unaffected by external interactions.

The dynamics of each isolated oscillator i is characterized by an internal variable $v_i(t)$, which increases until $V_u = \frac{2}{3}V_M$, decreases until $V_l = \frac{1}{3}V_M$, or remains constant at V_l during the charging, discharging, or resting stages, respectively, where V_M is a constant value. This variable is complemented by the binary function $y_i(t; n_i)$ that determines the type of oscillator by n_i (number of spikes per burst) and its stage: active when $y_i(t; n_i) = 1$, resting when $y_i(t; n_i) = 0$. Specifically, the dynamics is described by the following equations:

$$\begin{aligned} \dot{v}_i(t) &= \left[\frac{\ln 2}{T_{c,i}}\left(V_M - v_i(t)\right)\epsilon_i(t) - \frac{\ln 2}{T_{d,i}} v_i(t)\left(1 - \epsilon_i(t)\right)\right] y_i(t; n_i) \\ y_i(t; n_i) &= \sum\nolimits_{k=0}^{M_i(t)} \left[H(t - kT_{p,i} - \Delta\Phi_i) - H(t - (k+1)T_{p,i} + T_{s,i} - \Delta\Phi_i)\right] \end{aligned} \tag{1}$$

where $T_{p,i}$ is the total duration of the phrase (complete cycle), $M_i(t)$ is an integer obtained from the integer division of t by $T_{p,i}$ (in other words, the number of considered phrases), H is the Heaviside step function, and $\Delta\Phi_i$ is a phase delay that plays the role of an initial condition. The parameters $T_{c,i}$, $T_{d,i}$, and $T_{s,i}$ indicate the duration of the charging, discharging, and resting stages and determine the value of the phrase as follows: $T_{p,i} = T_{s,i} + n_i(T_{c,i} + T_{d,i})$. These parameters, illustrated in Fig 2, assume different values depending on the type of oscillator. For BOs, the durations of the phrase, as well as the resting, charging, and discharging stages, are denoted as $T_{p,m}$, $T_{s,m}$, $T_{c,m}$, and $T_{d,m}$, respectively. In the case of NBOs, these parameters are instead given by $T_{p,f}$, $T_{s,f}$, $T_{c,f}$, and $T_{d,f}$. However, the primary distinction between the two types of oscillator lies in the value of $n_i \in \mathbb{N}$, which is $n_m > 1$ for BOs and 1 for NBOs. Consequently, given the dependence of $T_{p,i}$ on n_i, the dynamics of the oscillators strongly depend on the number of spikes per burst. In summary, $v_i(t)$ expresses the spiking dynamics,

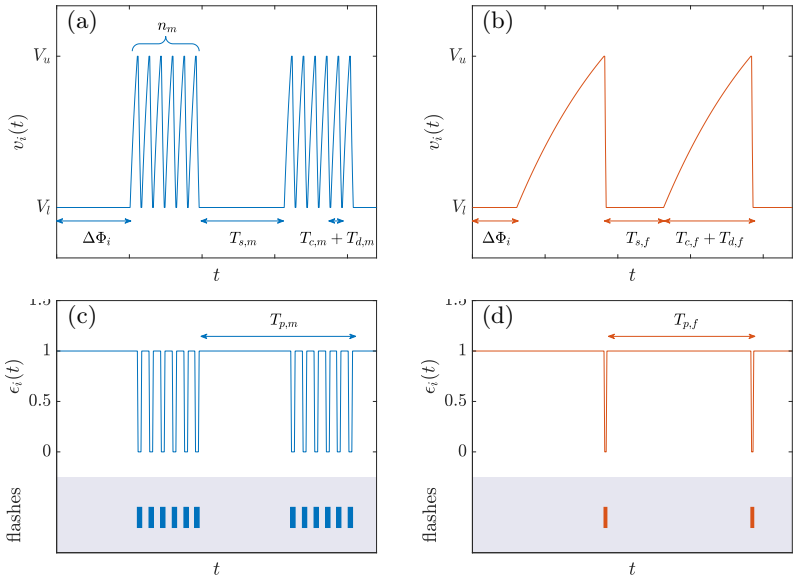

Fig. 2. Dynamics of a BO (a) and the corresponding evolution of $\epsilon_i(t)$ (c). Dynamics of a NBO (b) and the corresponding evolution of $\epsilon_i(t)$ (d).

while $y_i(t; n_i)$ describes the difference between BOs and NBOs through the fact that n_i is different among them, and enables the existence of the resting time $T_{s,i}$.

Going in-depth on the dynamical description, during the active stage, the dynamic $v_i(t)$ is given by two terms: the first ruling the charging stage, identified by $\epsilon_i(t) = 1$, and the second one regulating the discharging term identified by $\epsilon_i(t) = 0$. The binary variable $\epsilon_i(t)$ determines thus if the active oscillator is charging or discharging. The temporal evolution of $\epsilon_i(t)$ is given by:

$$\epsilon_i(t^+) = \epsilon_i(t) - \epsilon_i(t)H(v_i(t) - V_u) + (1 - \epsilon_i(t))H(V_l - v_i(t))\,, \tag{2}$$

which indicates that $\epsilon_i(t)$ switches to 0 when $v_i(t)$ reaches the upper threshold V_u, and switches to 1 when $v_i(t)$ reaches the lower threshold V_l, and keeps this value for $T_{s,i}$ time units, i.e., for all $t^+ \in [t, t + T_{s,i}]$.

In Fig. 2, we report the temporal behavior of $v_i(t)$ for both an isolated BO (Fig. 2(a)) and NBO (Fig. 2(b)) oscillator, together with the binary function $\epsilon_i(t)$ and the associated flashing event (Fig. 2(c) for BO and Fig. 2(d) for NBO) denoted by a rectangular mark displayed each time a flash is emitted.

Let C_m, resp. C_f, be the sets identifying the BOs, resp. the NBOs. When $N = |C_m| + |C_f|$ oscillators interact with each other, the dynamical equations are modified as follows. Once an oscillator $i \in C_m$, in the active stage, receives signals from other units, then the derivative of $v_i(t)$ increases. The opposite holds true for NBOs, namely once $i \in C_f$ in the active stage, the signals from the group decrease the derivative of $v_i(t)$. This different behavior can be cast

into the following form for $i = 1, \ldots, N$:

$$\begin{aligned} \dot{v}_i(t) &= \left[\frac{\ln 2}{T_{c,i}} \left(V_M - v_i(t) \right) \epsilon_i(t) - \frac{\ln 2}{T_{d,i}} v_i(t) \left(1 - \epsilon_i(t) \right) + \gamma_i(t) \right] z_i(t; n_i) \\ z_i(t; n_i) &= H(t - \Delta\Phi_i) + \sum\nolimits_{k=1}^{M_i'(t)} \left[H(t - t_{k,i} - T_{s,i}) - H(t - t_{k,i}) \right] \ , \end{aligned} \tag{3}$$

where $\gamma_i(t)$ is the coupling term, $z_i(t; n_i)$ determines the oscillator stage when coupled ($z_i(t; n_i) = 0$ during the resting stage, $z_i(t; n_i) = 1$ during the active stage) and $t_{k,i}$ is the time instant at which, for the $k-$th time, the following conditions are satisfied:

$$\textbf{(i)} \quad \mod \left(\eta_i(t), n_i \right) = 0 \ , \ \textbf{(ii)} \ v_i(t) = V_l \text{ and } \textbf{(iii)} \ \epsilon_i(t) = 0 \ . \tag{4}$$

with $\eta_i(t)$ being the number of peaks reached by $v_i(t)$ in the time interval $[0, t]$, and $n_i = n_m$ if $i \in C_m$ and 1 otherwise. The term $M_i'(t)$ indicates the number of times these three conditions are satisfied in the time interval $[0, t]$. Notice that in this case, the oscillator stage is not determined by the function $y_i(t; n_i)$ since, due to the coupling, the complete cycle of the oscillator no longer has a constant duration. The coupling term is expressed as:

$$\gamma_i(t) = \theta_i \sigma_i \sum\nolimits_{j=1}^{N} a_{ij} (1 - \epsilon_j(t)) \, , \tag{5}$$

where σ_i is the coupling strength, a_{ij}, $i, j = 1, \ldots, N$, are the entries of the adjacency matrix of the interaction graph, and θ_i is a term that assumes the value of 1 if $i \in C_m$, -1 otherwise. This models the fact that the coupling term, when non-zero and when the oscillator is in the active stage, affects the rate of change of $v_i(t)$. Specifically, when i is in the charging stage, $T_{c,i}$ decreases if i is a BO, and increases otherwise. Conversely, when i is in the discharging stage, $T_{d,i}$ increases if i is a BO, and decreases otherwise.

Notice that the coupling is defined in terms of the variable $\epsilon(t)$, in particular when $\epsilon_j(t) = 0$, i.e., the j-th oscillator is flashing, the latter influences the i-th one. Let us observe that in the rest of this work, we assume the interaction graph to be undirected and fully connected, namely each robot can potentially communicate with all the others.

In the mathematical model, two scenarios have been considered: one where the oscillators are stationary and interact through an unweighted adjacency matrix, and another where the oscillators are mobile and interact through a weighted time-varying interaction graph, with the weights depending on the distance between agents [15]. In both cases, the coupling strength is uniform across all agents, i.e., $\sigma_i = \sigma$ for all i. In this work, we focus on a scenario where the units are stationary and interact through an unweighted adjacency matrix, but the coupling strength depends on the type of oscillator: $\sigma_i = \sigma_m$ if $i \in C_m$ and $\sigma_i = \sigma_f$ if $i \in C_f$.

In the following we will focus on the configurations of oscillators given by:

1. *Mutually Coupled NBOs*: In this case, N NBOs interact among themselves.

2. *Mutually Coupled BOs*: This configuration considers interacting N BOs.
3. *Leader (BO) - Follower (NBO)*: In this configuration, both BOs and NBOs are present. The BOs are identical but do not interact with other units ($\sigma_m = 0$), whereas the NBOs interact among themselves and are influenced by the BOs ($\sigma_f \neq 0$). Notice that the condition $\sigma_m = 0$ implies that the dynamics of the BOs is described by Eq. (1).
4. *Mutually Coupled BOs and NBOs*: Here, both BOs and NBOs interact with each other and their behavior is governed by Eq. (3).

In [30] it is shown that: BOs can synchronize among them, NBOs cannot for any values of σ_i, and when BOs and NBOs are mingled, BOs can still synchronize and their synchronization induces the response of NBOs.

4 Robotic implementation

This section aims to introduce the implementation of the mathematical model (3) in the robots and the technical details we had to consider and resolve.

During the experiments, the robots remain stationary and, based on the values of the parameters (θ_i, σ_i, $T_{c,i}$, $T_{d,i}$, $T_{s,i}$, V_M, n_i, $\Delta\Phi_i$) loaded from a file stored on their memory, they are assigned either to BO, i.e., "male", or to NBO, i.e., "female". At each time step $t_h = ht_s$ ($h = 1, 2, \ldots$), each robot updates its state variable by performing an integration step of Eq. (3), by using the 4th-order Runge-Kutta method with a fixed step size of Δt. The robot then updates the value of $\epsilon_i(t_h)$ by using Eq. (2), and based on this value, it controls a green LED (activated if $\epsilon_i(t_h) = 0$, deactivated otherwise) and broadcast its current value of $\epsilon_i(t_h)$. Both $v_i(t_h)$ and $\epsilon_i(t_h)$ are recorded in a file stored inside the memory of each robot, that will be transmitted via Wi-Fi to a computer at the end of each experiment, to post-process the produced data.

To prevent time drift during integration, before starting each experiment, the computer sends a file to the robots containing an absolute reference time, t_{ref}. This ensures that, at the beginning of the experiment, the robots, equipped with a universal clock, start their integration process once $t \geq t_{ref}$. As a result, the robots will perform the integration steps at times $t = t_{ref} + ht_s$ for $h = 1, \ldots, T/t_s$, where T denotes the total duration of the experiment.

In the mathematical model, the interaction graph is fully connected. On the other hand, in the experiment the neighbor detection relies on local communication provided by the range & bearing board, with a transmission power set to enable communication between robots up to a distance of $40\,[cm]$, to minimize battery consumption. Given that the communication system is not immune to message loss and message corruption, the neighborhood of the robot i is defined as follows:

$$\mathcal{N}_i(t_h) = \{j : \text{a valid message from } j \text{ is received by } i \text{ in } t' \in]t_{h-1}, t_h]\}$$

where "valid" refers to messages that are not corrupted due to interference or that do not come from previous time steps or by the robot itself. To ensure

the reliability of communication, the robots broadcast messages containing information that allows the receiving robots to check their validity. Specifically, the message, consisting of two bytes, is structured as follows: the most significant byte contains the robot ID, i, which helps prevent the receiving robot from considering the same neighbor information multiple times during an integration step; the least significant byte is divided into 4-bit segments: the upper segment containing $r_i(t_h) = \mathrm{mod}(h, 5)$, and the lower one containing $\epsilon_i(t_h)$.

Each time a robot i receives a message from another unit j, it performs a set of checks, including:

- verifying that the message is not corrupted (for example, if $\epsilon_j(t_h)$ is different from 0 or 1 the message is considered corrupted;
- ensuring that the message comes from the current time step, i.e., $r_i(t_h) = r_j(t_h)$;
- checking that the sender j does not already belong to $\mathcal{N}_i(t_h)$.

If a message does not meet all these conditions, it will be neglected by the receiver. As a result, there is no guarantee that the adjacency matrix describing the interaction graph among the robots is time-constant and undirected. Consequently, the value of a_{ij} in Eq. (3) becomes time-varying, with $a_{ij}(t_h) = 1$ if and only if $j \in \mathcal{N}_i(t_h)$.

The elementary time step, t_s, must be chosen large enough to allow the robots to detect their neighbors but at the same time it cannot be too large, as the use of the range & bearing board can significantly drain the battery. To determine this value, we followed the same methodology adopted in [36]. Specifically, we conducted experiments by using $N = 2$ robots communicating at a distance $d = 15\,[cm]$ and we tested different values of t_s. During these experiments, robots continuously sent messages, and, at intervals of t_s, they recorded a value of 1 in a file if a message was received within the interval, or 0 otherwise. These files were then post-processed to compute the probability of message reception. The outcomes of these experiments are shown in Fig. 3(a), which depicts the likelihood of receiving messages as a function of t_s. Based on these findings, we select $t_s = 500\,[ms]$ which provides a message reception probability $p = 0.85$. Let us notice that this probability refers to the case in which communication occurs between two robots. Indeed, when the number of robots, N, increases, the value of p decreases, see Fig. 3(b) where we set $t_s = 500\,[ms]$. We also investigated the impact of the distance among the robots on the communication probability. For this purpose, we conducted experiments by using $N = 2$ robots and an elementary time step of $t_s = 500\,[ms]$; as shown in Fig. 3(c), the probability remains constant for distances from $d = 10\,[cm]$ to $d = 35\,[cm]$, after which it starts to decrease, reaching zero at $d = 45\,[cm]$. Let us observe that this behavior is expected, given that the transmission power of the robots is configured to allow communication up to a maximum distance of approximately $40\,[cm]$.

5 Experimental results

In this section, we present the results obtained from the experiments conducted by using the robotic implementation described in the previous section. Specifi-

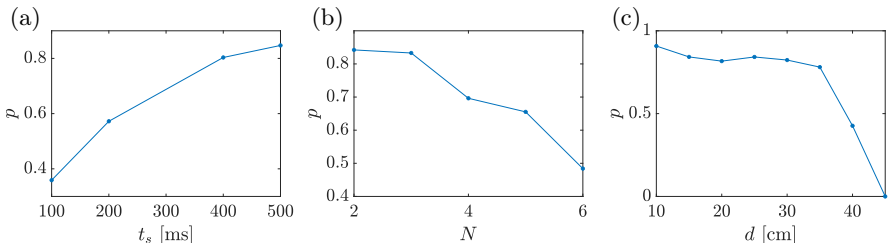

Fig. 3. Probability of receiving a non-corrupted message, p, as function of the elementary time step t_s (a), the number of robots N (b), and the distance among robots d (c). In panels (a) and (c), $N = 2$, whereas in panels (b) and (c), $t_s = 500\,[ms]$.

cally, we carried out four types of experiments: the first shows that the NBOs are not able to synchronize in the absence of BOs; the second demonstrates that BOs can achieve synchronization; the third characterizes the response of the NBOs to the BOs synchronization in a leader-follower configuration; and the fourth one investigates the NBOs response to BOs synchronization in a mutually coupled BO-NBO configuration.

We use the synchronization error, computed separately for BOs and NBOs, to evaluate the synchronization among the oscillators:

$$\delta_k(t) = \frac{1}{|C_k|} \sum\nolimits_{\substack{i,j \in C_k \\ j \neq i}} |v_i(t) - v_j(t)| \quad \text{for } k \in \{m, f\}\,,$$

$\delta_k(t)$ is small if the BOs, resp. NBOs, exhibit at time t close values of v_i.

The following parameters, based on previous studies involving real fireflies [31], were used in all experiments: $T_{c,m} = 0.5\,[s]$, $T_{d,m} = 0.2\,[s]$, $T_{s,m} = 5.8\,[s]$, $n_m = 6$, $T_{c,f} = 6\,[s]$, $T_{d,f} = 0.1\,[s]$, $T_{s,f} = 3.9\,[s]$, and $\Delta t = 0.05\,[s]$. Additionally, $V_M = 9$, resulting in $V_l = 3$ and $V_u = 6$. For the ODE integration, we used $\Delta t \neq t_s$, resulting in two distinct time scales: numerical and physical.

In the first experiment, lasting $T = 1000\,[s]$, $N = 2$ NBOs interact at a distance $d = 20\,[cm]$. Each oscillator is initialized to a different initial condition and, at each time step t_h, it integrates the ODE (3) with $\sigma_f = 2$. Fig. 4 shows the dynamics of the oscillators and the corresponding flashes, revealing that, despite starting from very similar initial conditions, the two oscillators do not synchronize. This demonstrates that, as in the mathematical model, NBOs cannot synchronize on their own, independently from the coupling strength value.

For the second experiment, a group of $N = 6$ BOs is arranged in a hexagonal formation with a radius $d_r = 20\,[cm]$, and interact with each other with a coupling strength $\sigma_m = 0.05$. The experiment lasts $T = 800\,[s]$ and, as shown in Fig. 5(a), the system reaches synchronization despite a reception probability estimated to be ~ 0.5, according to the results shown in Fig. 3(a). We compare this result with a numerical simulation where we introduced the parameter p to emulate the message loss characterizing the local communication provided by the range & bearing board. Specifically, at each time step, the coupling term

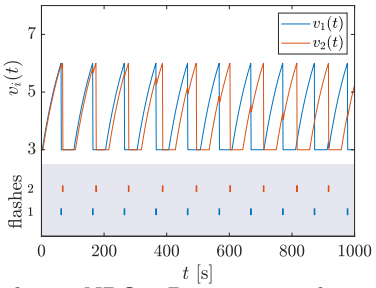

Fig. 4. Experimental results: 2 NBOs. Dynamics and corresponding flashes of two NBOs interacting at a distance of $d = 20\,[cm]$. Despite starting from very close initial conditions, the NBOs do not achieve synchronization.

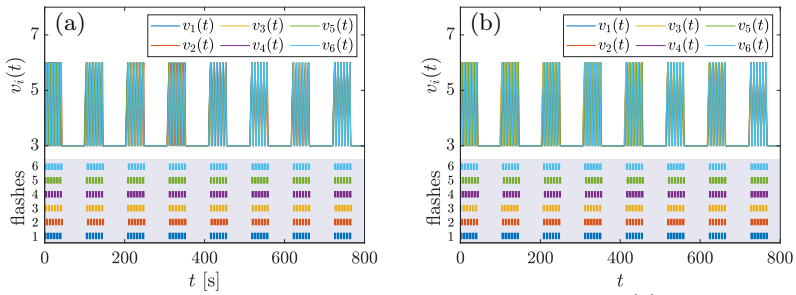

Fig. 5. Experimental and numerical results: 6 interacting BOs. (a) Dynamics of $N = 6$ interacting robots, each exhibiting a bursting oscillator, arranged in a hexagonal formation with a radius $d_r = 20\,[cm]$. (b) Results obtained from a simulation in which a probability of message reception $p = 0.5$ is considered. In both cases, a coupling strength $\sigma = 0.05$ has been used.

becomes $\gamma_i'(t) = \theta_i \sigma_i \sum_{j=1}^{N} \omega_{ij}(t)\,(1 - \epsilon_j(t))$, where $\omega_{ij}(t)$ takes the value 1 with probability p and 0 otherwise. We can observe (Fig. 5(b)) that the numerical results agree with the experimental ones.

The third set of experiments involves $N = 8$ oscillators, consisting of 6 BO and 2 NBO units. In particular, the BOs are arranged in a hexagonal formation, with the NBOs placed at $3\,[cm]$ from the center of the hexagon, facing each other. In each experiment, the distance between the center and the vertices of the hexagon, denoted by d_r, is kept constant but varies across experiments, being incrementally increased from one experiment to the next. In each experiment, the BOs start from the same initial condition and do not interact with any other units ($\sigma_m = 0$). As a result, they maintain synchronization throughout the entire experiment. Notice that, in this case, synchronization does not arise from coupling, but is due to the fact that the oscillators are identical as they have the same initial conditions. The NBOs, on the other hand, interact with each other and are susceptible to the BO state, with a coupling strength of $\sigma_f = 2$. Fig. 6(a) shows the total synchronization error among the NBOs computed as the norm of $\delta_f(t)$ over the time interval $\left[\frac{4}{5}T, T\right]$, i.e., we remove an initial transient. We can appreciate a low synchronization error for many values of d_r, i.e., up

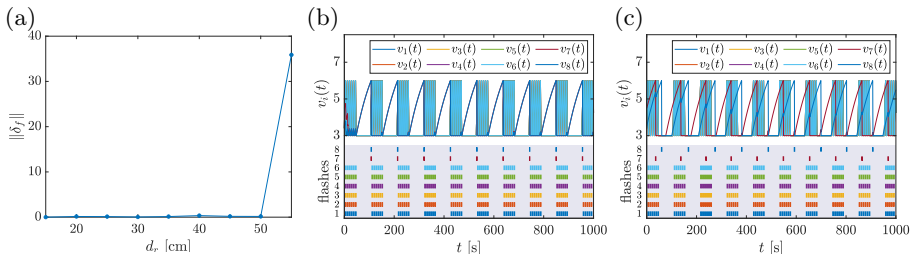

Fig. 6. Experimental results: 6 BOs (Leaders) and 2 NBOs (Followers). The experiments use the configuration in Fig. 1(b), with BOs arranged in a hexagon formation with a radius d_r and NBOs placed 3 cm from the center of the hexagon, facing each other. (a) Synchronization error of the NBOs as a function of the hexagon radius d_r. (b) Dynamics and corresponding flashes of the oscillators for $d_r = 20\,[cm]$, showing that the NBOs respond to synchronization after a short time. (c) Dynamics and corresponding flashes of the oscillators for $d_r = 55\,[cm]$, showing that NBOs do not synchronize.

to $d_r = 50\,[cm]$. For $d_r = 55\,[cm]$, however, the synchronization error is high, indeed the NBOs, being very far from the BOs, do not detect the latter. The dynamics of the oscillators and corresponding flashes for $d_r = 20\,[cm]$ and for $d_r = 55\,[cm]$ are shown in Fig. 6(b) and Fig. 6(c), respectively. We notice that, for $d_r = 20\,[cm]$, the NBOs respond to the synchronization and synchronize between themselves in a short time.

The fourth experiment also includes $N = 8$ oscillators: 6 BOs arranged in a hexagonal formation with radius $d_r = 25\,[cm]$ and 2 NBOs placed at $2\,[cm]$ from the center facing each other. We hereby consider a scenario in which BOs and NBOs start from different initial conditions and interact among themselves. Specifically, the BOs interact with a coupling strength of $\sigma_m = 0.5$, while the NBOs have a coupling strength of $\sigma_f = 2$. The response to synchronization in NBOs occurs once the BOs synchronize among themselves, i.e., about at $t \sim 1000\,[s]$ or 10 bursts of the BOs. Fig. 7 shows the time evolution of the oscillators state variables and the corresponding flashes.

6 Conclusions

In this work, we used a team of e-puck2 robots to implement and validate the mathematical model discussed in [30], describing the response to synchronization in fireflies. The model considers a heterogeneous system composed of two types of oscillators: NBOs, representing females unable to synchronize alone, and BOs, representing males capable of achieving synchronization by their own. Specifically, the model focuses on the phenomenon of response to synchronization, where NBOs synchronize as a result of their interactions with synchronous BOs, demonstrating how heterogeneity can induce coordinated behavior in multi-agent systems.

For robotic implementation, we considered two populations of robots: one representing BOs and the other representing NBOs. Such implementation is

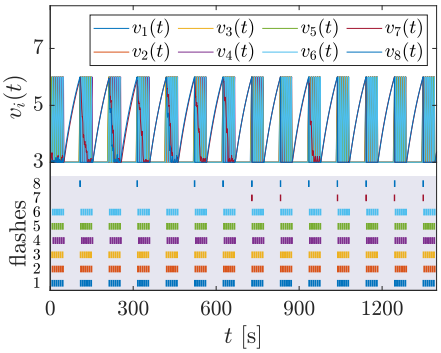

Fig. 7. Experimental results: 6 BOs and 2 NBOs. The experiment employs the same configuration used for Fig. 6, with $d_r = 25\,[cm]$ and the NBOs placed at $2\,[cm]$ from the center. The BOs interact with a coupling strength $\sigma_m = 0.5$ and the NBOs with $\sigma_f = 2$. Each oscillator starts from different initial conditions. The figure shows the time evolution of the oscillators state variables and their corresponding flashes.

fully distributed as the robots integrate their own dynamics and locally interact through the range & bearing board. The experiments explored various configurations. In more detail, using a configuration consisting only of NBOs in absence of BOs, we demonstrated that, despite starting from nearly identical initial conditions, they are unable to synchronize on their own. We also tested interacting BOs, confirming their ability to achieve synchronization. Additionally, we investigated both leader-follower (BOs acting on NBOs) and interacting BOs and NBOs configurations to study the response of the NBOs to the BO synchronization, proving that the NBOs can synchronize in the presence of the BOs. Through our experiments, we reproduced the main features of the mathematical model, proving its robustness against real-world factors, including message loss during communication or corrupted messages.

The validation of this model offers insight into practical applications involving units that are not capable of synchronizing alone. Indeed, the introduction of additional units capable of synchronizing could induce synchronization among the non-synchronizing units. Although our study focused on static robots, future work will extend this investigation by considering mobile robots, allowing us to explore the impact of units' motion on the response to synchronization. Additionally, future research could investigate the influence of varying the number of NBOs and BOs on the synchronization response, by studying how closely the observed results reflect real-world behavior.

Acknowledgments. C. Tomaselli acknowledges support by the Namur Institute for Complex Systems (naXys) and by the University of Catania for her visiting period at the University of Namur. The research of C. Tomaselli and L.V. Gambuzza has been framed and supported by University of Catania under the PIA.CE.RI. project, starting grant for RTDb. G. M. Ramírez-Ávila acknowledges the European Union's Horizon 2020 research and innovation program under the Marie Sklodowska-Curie grant agreement No 101034383.

Disclosure of Interests. The authors have no competing interests to declare that are relevant to the content of this article.

References

1. Aihara, I., Takeda, R., Mizumoto, T., Otsuka, T., Takahashi, T., Okuno, H.G., Aihara, K.: Complex and transitive synchronization in a frustrated system of calling frogs. Physical Review E **83**(3), 031913 (2011)
2. Backwell, P.R.Y.: Synchronous waving in fiddler crabs: a review. Current Zoology **65**(1), 83–88 (2019)
3. Balanov, A., Janson, N., Postnov, D., Sosnovtseva, O.: Synchronization: From Simple to Complex. Springer Berlin, Berlin (2007)
4. Boccaletti, S., Pisarchik, A.N., del Genio, C.I., Amann, A.: Synchronization: From Coupled Systems to Complex Networks. Cambridge University Press, Cambridge (2018)
5. Buck, J., Buck, E.: Flash synchronization as tool and as enabler in firefly courtship competition. The American Naturalist **116**(4), 591–593 (1980)
6. Buck, J.B.: Synchronous flashing of fireflies experimentally induced. Science **81**(2101), 339–340 (1935)
7. Carlson, A.D., Copeland, J., Raderman, R., Bulloch, A.G.M.: Response patterns of female photinus macdermotti firefly to artificial flashes. Animal Behaviour **25**, 407–413 (1977)
8. Copeland, J., Moiseff, A.: Flash precision at the start of synchrony in photuris frontalis. Integrative and Comparative Biology **44**(3), 259–263 (2004)
9. Cratsley, C.K.: Flash signals, nuptial gifts and female preference in photinus fireflies. Integrative and Comparative Biology **44**(3), 238–241 (2004)
10. De Cock, R., Faust, L., Lewis, S.: Courtship and mating in phausis reticulata (coleoptera: lampyridae): male flight behaviors, female glow displays, and male attraction to light traps. The Florida Entomologist **97**(4), 1290–1307 (2014)
11. Dunning, D.C., Byers, J.A., Zanger, C.D.: Courtship in two species of periodical cicadas, magicicada septendecim and magicicada cassini. Animal Behaviour **27**, 1073–1090 (1979)
12. Ercsey-Ravasz, M., Sárközi, Z., Néda, Z., Tunyagi, A., Burda, I.: Collective behavior of electronic fireflies. The European Physical Journal B **65**(2), 271–277 (2008)
13. Faust, L.F.: Natural history and flash repertoire of the synchronous firefly photinus carolinus (coleoptera: Lampyridae) in the great smoky mountains national park. Florida Entomologist pp. 208–217 (2010)
14. Faust, L.F.: Fireflies, Glow-worms, and Lightning Bugs: Identification and Natural History of the Fireflies of the Eastern and Central United States and Canada. University of Georgia Press, Athens, Georgia (2017)
15. Fujiwara, N., Kurths, J., Díaz-Guilera, A.: Synchronization in networks of mobile oscillators. Physical Review E **83**(2), 025101 (2011), `http://link.aps.org/doi/10.1103/PhysRevE.83.025101`
16. Hartbauer, M., Römer, H.: A novel distributed swarm control strategy based on coupled signal oscillators. Bioinspiration & Biomimetics **2**(3), 42 (2007)
17. Kousaka, T., Kawakami, H., Ueta, T.: Synchronization of electric fireflies by using square wave generators. IEICE transactions on fundamentals of electronics, communications and computer sciences **81**(4), 656–663 (1998)
18. Lloyd, J.E.: Fireflies of melanesia: Bioluminescence, mating behavior, and synchronous flashing (coleoptera: Lampyridae). Environmental Entomology **2**(6), 991–1008 (1973)

19. Maquitico, Y., Coronado, J., Luna, A., Vergara, A., Cordero, C.: Deceptive seduction by femme fatale fireflies and its avoidance by males of a synchronous firefly species (coleoptera: Lampyridae) (2024)
20. McCrea, M., Ermentrout, B., Rubin, J.E.: A model for the collective synchronization of flashing in photinus carolinus. Journal of The Royal Society Interface **19**(195), 20220439 (2022)
21. Michaelidis, C.I., Demary, K.C., Lewis, S.M.: Male courtship signals and female signal assessment in photinus greeni fireflies. Behavioral Ecology **17**(3), 329–335 (2006)
22. Mirollo, R.E., Strogatz, S.H.: Synchronization of pulse-coupled biological oscillators. SIAM Journal on Applied Mathematics **50**(6), 1645–1662 (1990)
23. Moiseff, A., Copeland, J.: Firefly synchrony: a behavioral strategy to minimize visual clutter. Science **329**(5988), 181–181 (2010)
24. Nelson, S., Carlson, A.D., Copeland, J.: Mating-induced behavioural switch in female fireflies. Nature **255**(5510), 628–629 (1975)
25. Nityananda, V., Balakrishnan, R.: Leaders and followers in katydid choruses in the field: call intensity, spacing and consistency. Animal Behaviour **76**(3), 723–735 (2008)
26. Peleg, O.: A new chapter in the physics of firefly swarms. Nature Reviews Physics **6**(2), 72–74 (2024)
27. Perez Diaz, F.: Firefly-inspired synchronization in swarms of mobile agents. Ph.D. thesis, University of Sheffield (2016)
28. Pikovsky, A., Rosenblum, M., Kurths, J., Synchronization, A.: A universal concept in nonlinear sciences. Self **2**, 3 (2001)
29. Rabha, M.M., Sharma, U., Goswami, A., Gohain Barua, A.: Bioluminescence emissions of female fireflies of the species luciola praeusta. Journal of photochemistry and photobiology. B, Biology **170**, 134–139 (2017)
30. Ramírez-Ávila, G.M., Kurths, J.: Unraveling the primary mechanisms leading to synchronization response in dissimilar oscillators. The European Physical Journal Special Topics **225**, 2487–2506 (2016)
31. Ramírez-Ávila, G.M., Deneubourg, J.L., Guisset, J.L., Wessel, N., Kurths, J.: Firefly courtship as the basis of the synchronization-response principle. EPL (Europhysics Letters) **94**(6), 60007 (2011)
32. Ramírez-Ávila, G.M., Kurths, J., Deneubourg, J.L.: Fireflies: A Paradigm in Synchronization, pp. 35–64. Springer International Publishing, Cham (2018)
33. Ramírez-Ávila, G.M., Kurths, J., Depickère, S., Deneubourg, J.L.: Modeling Fireflies Synchronization, pp. 131–156. Springer International Publishing, Cham (2019)
34. Sarfati, R., Hayes, J.C., Peleg, O.: Self-organization in natural swarms of photinus carolinus synchronous fireflies. Science Advances **7**(28), eabg9259 (2021)
35. Tomaselli, C., Guastella, D.C., Muscato, G., Minati, L., Frasca, M., Gambuzza, L.V.: Synchronization of moving chaotic robots. IEEE Robotics and Automation Letters **9**(7), 6496–6503 (2024)
36. Tomaselli, C., Guastella, D.C., Muscato, G., Frasca, M., Gambuzza, L.V.: A multi-robot system for the study of face-to-face interaction dynamics. IEEE Robotics and Automation Letters (2023)
37. Trianni, V., De Simone, D., Reina, A., Baronchelli, A.: Emergence of consensus in a multi-robot network: from abstract models to empirical validation. IEEE Robotics and Automation Letters **1**(1), 348–353 (2016)
38. Vencl, F.V., Blasko, B.J., Carlson, A.D.: Flash behavior of female photuris versicolor fireflies (coleoptera: Lampyridae) in simulated courtship and predatory dialogues. Journal of Insect Behavior **7**(6), 843–858 (1994)